Available online at www.eccomasproceedia.org
Eccomas Proceedia COMPDYN (2023) 5258-5272

ECCOMAS
Proceedia

COMPDYN 2023
9th ECCOMAS Thematic Conference on
Computational Methods in Structural Dynamics and Earthquake Engineering
M. Papadrakakis, M. Fragiadakis (eds.)
Athens, Greece, 12-14 June 2023

REDUCED ORDER MODELS TO ESTIMATE SEISMIC RISK OF UNREINFORCED MASONRY DWELLINGS

Ana M. Zapata-Franco[1], **Yeudy F. Vargas-Alzate** [2], **José R. Gonzalez-Drigo** [3] **and Rodolfo J. Tirado-Gutiérrez** [4]

[1,2,4] Department of Civil and Environmental Engineering. Universitat Politècnica De Catalunya
Jordi Girona, 1-3, 08034, Barcelona, Spain
{ana.maria.zapata, yeudy.felipe.vargas, rodolfo.javier.tirado}@upc.edu

[3] Department of Structural Engineering. Universitat Politècnica De Catalunya
Jordi Girona, 1-3, 08034, Barcelona, Spain
jose.ramon.gonzalez@upc.edu

Abstract

In order to estimate seismic risk at an urban level it is necessary to consider several sources of uncertainty. However, the higher the uncertainties related to both structural modelling and seismic hazard, the higher the computational time to extract reliable information to assess seismic risk. Thus, simplifying the structural model significantly diminishes the computational effort, allowing analyzing several building models in a fraction of time. In this sense, one of the most simplified representations to approximate the horizontal dynamic response of a structure is the Single Degree of Freedom system (SDoF). It allows calculating time-history responses in an easy way, given a determined fundamental period and damping. Though, the response of an SDoF does not consider neither the stiffness' loss because of plastic damage nor the participation of higher modes. Advanced intensity measures (IMs) look for addressing these shortcomings by averaging spectral quantities around the fundamental period (T_1) of the analyzed building. Analogous to this approach, it is proposed to estimate the dynamic response of a building by averaging the time history response of a set of SDoF systems with periods in the interval ($0.1T_1$, $1.8T_1$). The dynamic response associated with each of them has been estimated by means of the dynamic equilibrium equation for SDoF systems. In order to verify the efficiency of the proposed approach, it has been analyzed the dynamic behavior of unconfined masonry. This structural type is very prone to damage during an earthquake, as it has poor seismic performance. Observed damage and consequences of a catastrophic event occurred in Colombia (1999) have been used to verify the methodological approach.

Keywords: Single degree of freedom, unconfined masonry, seismic risk, Monte Carlo simulations.

ISSN:2623-3347
Peer-review under responsibility of the organizing committee of COMPDYN 2023.
doi: 10.7712/120123.10798.21097

1 INTRODUCTION

Seismic risk mainly depends on the capacity of civil infrastructure to withstand ground motions produced by earthquakes. Current strategies to mitigate this inherent risk to society are oriented to improve design methodologies for new structures and to quantify the expected performance of existing ones. In turn, innovative technologies are implemented day by day to improve this performance.

This research aims to characterize the vulnerability and fragility of Unreinforced Masonry Structures, URMM, by creating a simplified model that allows numerous calculations to be performed in a short time. To this end, it has been decided to use the combined response of a set of single-degree-of-freedom (SDoF) systems. This type of model allows the time-history response of a structure to be approximated with less computational effort. Specifically, to account for plastic damage and the involvement of higher modes, the dynamic response was approximated by averaging the response of a set of SDoFs around the fundamental period of the simulated structures [1]. This period has been obtained through classical relationships in terms of power functions, which depend on the height of the structure (see for instance Martins & Silva, 2021 [2]).

Once the structural models were obtained, the next step was to calculate engineering demand parameters (EDPs), which can be used to obtain fragility curves. These EDPs were estimated by assuming that the fundamental period of the structures varies randomly. Then, clouds of IM-EDP points in log-log space were used to identify the most efficient IMs. Based on these, fragility functions have been derived for the URMM structure typology [3]; cloud analysis has been used to this end [4]. In short, a regression line is obtained from the IM-EDP relationship that is used to calculate the mean of a parametric statistical distribution given an IM. The variation of this distribution is estimated from the standard deviation of the bivariate distribution (IM-EDP) set with respect to the fitted curve, allowing estimating the probability of exceeding a given damage threshold.

To validate the fragility curves obtained, two scenarios are proposed to estimate the number of people that could be affected after a strong ground motion event. In the first case, the simulation of the different structures is carried out with a participation factor (PF_1) variable according to the height of the floor, and in the second case, the PF_1 is kept constant for all floors, as specified in Martins & Silva, 2021 [5]. After obtaining these fragility curves, the number of people affected is estimated and compared with the data observed after a real catastrophic event, such as the 1999 Armenia earthquake in the coffee region of Colombia [6]. Based on these results, it has been analyzed which of the two simulated scenarios presents a better fit with reality.

2 STRUCTURAL MODELLING

URMM typology has been and continues to be a dangerous solution to meet the need for affordable housing in developing countries, especially in areas with moderate to high seismic risk. In the specific case of Colombia, this type of housing is typical in urban and rural areas and represents approximately 60% of the existing housing in the country. In there, one can find URMM structures whose number of stories varies from 1 to 5; the typical height is 2.4 m. This type of construction is very susceptible to damage during an earthquake since it has a low seismic performance. It is worth mentioning that sometimes residents unintentionally increase this vulnerability by making inappropriate modifications to their homes. These modifications are usually made to increase the size of the dwelling. Historically, the inhabitants of other countries in the world have also used this typology, with the consequent increase in seismic risk [7]. In earthquake-prone areas, there are many regulations for new construction. In these areas, URMM dwellings are generally forbidden due to its high vulnerability. Nevertheless, this type of construction is cheap and is used by a significant number of families with limited resources. This exacerbates the overall picture of seismic risk in Colombia [3].

2.1 Surrogate model based on the combined response of single degree of freedom systems.

In order to analyze the expected damage of URMM buildings, it is necessary to consider several sources of uncertainty [5,8]. However, the more complex the structural model, the more computation time is required to extract reliable information from it. Therefore, simplifying the structural model significantly reduces the computational effort, allowing multiple building models to be analyzed in a fraction of the time.

In this sense, one of the most simplified representations of a building is an SDoF system. This model has been extensively used to estimate the dynamic response of civil structures [5]. It allows calculating time-history responses in an easy way, given a determined fundamental period and damping. However, the response of a single SDoF does not consider the loss of stiffness due to plastic damage, nor the participation of higher modes.

In the development of advanced proxies based on seismic intensity measures (IMs) for estimating engineering demand parameters, EDPs, these shortcomings have been addressed by averaging spectral quantities around the fundamental period of the building model. Analogous to this approach, it is proposed to approximate the dynamic response of a URMM building, in each principal direction, by averaging the time-history response of a set of SDoF systems in the interval ($0.1T_n$, $1.8T_n$); where T_n represents the fundamental period of the analyzed building.

Thus, the dynamic response associated with each oscillator has been estimated by means of the dynamic equilibrium equation for SDoF systems:

$$m\ddot{u}_n(t) + c\dot{u}_n(t) + ku_n(t) = -m\ddot{u}_{g,n}(t) \tag{1}$$

where $\ddot{u}_n(t)$, $\dot{u}_n(t)$, and $u_n(t)$ are the spectral acceleration, velocity and displacement time history responses of the SDoF in the n direction, respectively; $\ddot{u}_{g,n}(t)$ is the acceleration ground motion; m, c, and k represent the mass, damping, and stiffness of the system, respectively. Thus, the spectral time history response of a building in the n direction (x or y) can be estimated as follows:

$$\ddot{u}_n(t) = \frac{1}{p}\sum_{i=1}^{p} \ddot{u}(t, T_i) \tag{2}$$

$$\dot{u}_n(t) = \frac{1}{p}\sum_{i=1}^{p} \dot{u}(t, T_i) \tag{3}$$

$$u_n(t) = \frac{1}{p}\sum_{i=1}^{p} u(t, T_i) \tag{4}$$

where T_i are the components of a vector of ten periods equally spaced within the interval (0.1Tx, 1.8Tx) for the x and (0.1Ty, 1.8Ty) for the y directions. In this way, the 3D spectral time history response in terms of acceleration, velocity and displacement of the simulated system has been estimated as follows:

$$\ddot{u}_{(x,y)} = \sqrt{\ddot{u}_x^2 + \ddot{u}_y^2} \tag{5}$$

$$\dot{u}_{(x,y)} = \sqrt{\dot{u}_x^2 + \dot{u}_y^2} \tag{6}$$

$$u_{(x,y)} = \sqrt{u_x^2 + u_y^2} \tag{7}$$

For the sake of simplicity, it has been omitted to write explicitly the dependence of the response variables on time in these equations.

2.2 Maximum global drift ratio as EDP

Several EDPs can be extracted from the averaged time-history responses described in the previous section. For example, the maximum global drift ratio of a structure, MGDR, which is an EDP that is widely used in seismic risk estimation using the capacity spectrum method [9], can be estimated according to the following equation:

$$MGDR = PF_1 \frac{max\,(u_{(x,y)})}{\mathrm{H}} \tag{8}$$

where PF_1 is the load participation factor [10]; H is the height of the building. Regarding PF_1, it has been assumed that this variable is a function of the number of stories as depicted in Figure 1. In summary, $PF_1 = (\frac{N_{st}}{10} + 0.9)$, where N_{st} represents the number of stories.

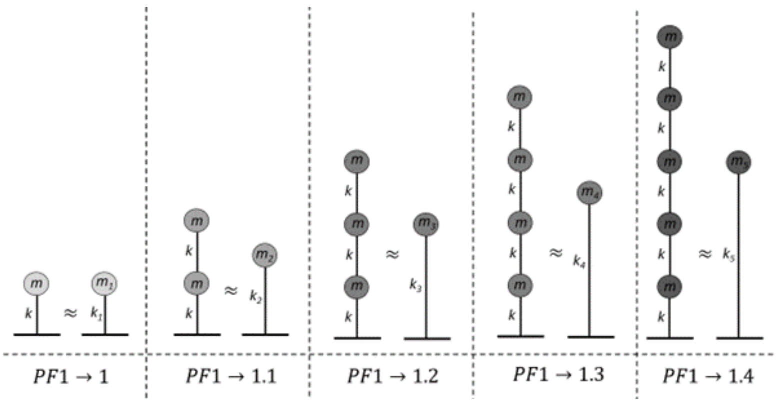

Figure 1: Variation of $\boldsymbol{PF_1}$ depending on the higher of stories.

3 SEISMIC HAZARD CHARACTERIZATION

3.1 Database of ground motion records

Figure 2 shows the classification of the Colombian territory into three levels of seismic hazard: high in red, medium in yellow, and low in green. These were determined based on historical and instrumental seismic information provided by the National Seismological Network.

In this research, a compilation has been made of the ground motions recorded between 1993 and 2017, with a magnitude greater than 4.0 Mw within Colombia. These records have been extracted from the SGC [11]. A total of 1992 records have been obtained, which have been used to make better statistics, reduce the uncertainty of the data, and provide a better adaptation to the seismogenic conditions of the Colombian territory.

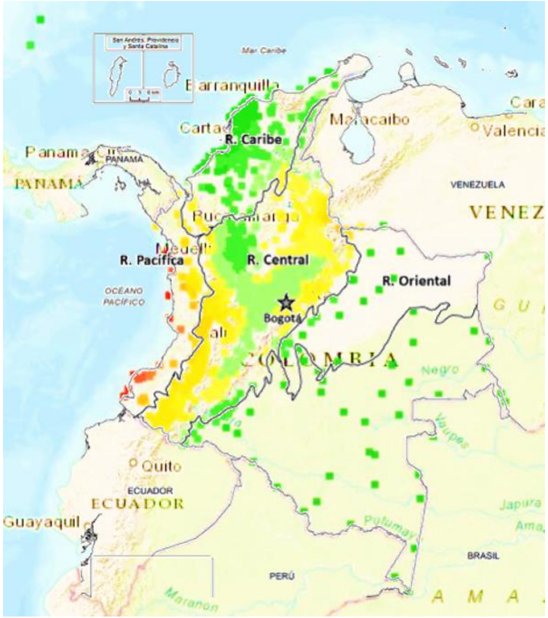

Figure 2: Colombian Seismic Hazard map for PGAs (Image taken from SGC) [11]

The ground motion records were divided into two groups according to the ground conditions in which they were acquired. The first corresponds to signals recorded on bedrock, from which a total of 1236 records were identified. The second group are signals recorded on less rigid ground, with a total of 756 records. For both types of records, environmental noise and other disturbances that could affect the quality of the signal were identified and corrected. A MATLAB code was developed for this purpose. Figure 3 shows the geometric mean of the horizontal spectra of the resulting ground motion records.

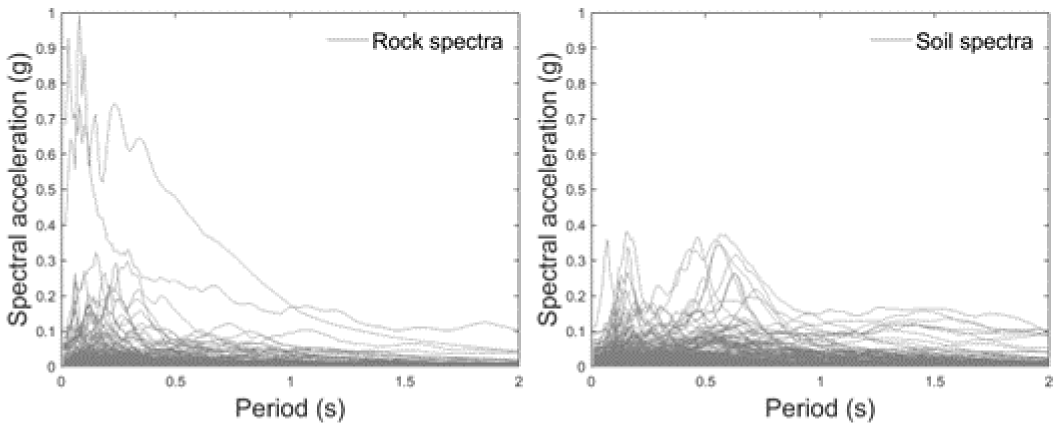

Figure 3: Spectra of the selected records. Above: Geometric Mean Spectra of the horizontal components (Left: Rock Right: Soil). Bottom: Median (Left) and percentile 95 (Right) of the entire set of spectra

3.2 Scaling ground motion records

In this article, seismic risk has been quantified in a probabilistic manner. Therefore, fragility functions based on the cloud analysis have been derived [4]. This methodology requires obtaining pairs of points that represent the seismic hazard (in terms of IMs) and the structural response (EDPs). These points have been obtained through time-history analysis by considering uncertainties in the structural modelling. Consequently, the seismic hazard has been characterized by using a probabilistic set of ground motion records.

There are several methodologies to scale ground motions from a database [12]. Typically, the goal is to find a significant set of records leading the structure to multiple performance levels. However, as indicated by the well-known Richter's law, the number of high-intensity ground motion records is much smaller than the number of low-intensity ones [13]. To mitigate these issues when employing cloud analysis, the procedure employed in Vargas-Alzate et al., 2022 [14] has been used for selecting and scaling (where necessary) ground motion records. In short, this procedure attempts to scale a set of data sets uniformly across a series of intervals of increasing intensity with the goal of minimizing the scale factor. To do so, an IM identified as AvSa is considered herein to perform the selection and scaling of the records. Note that AvSa is calculated as the arithmetic mean of spectral acceleration values around the fundamental period of the analyzed system. Moreover, because of the 3D approach in modelling, AvSa is calculated from the geometric mean of the horizontal spectra.

The period range for averaging the spectral ordinates of the IM should be established from the dynamic properties of the entire population of buildings [1]. Accordingly, this range has been set at (0.1-0.71) sec. This period range will be justified in the next section. The intensity levels defining the upper and lower limits of each band range from 0.2 to 2.0 g at intervals of 0.2 g (i.e., 10 bands have been defined).

Thus, the horizontal components of 1000 ground motion records acquired at the bedrock (100 per band) have been obtained from the seismic database whilst 700 (70 per band) for those recorded at soil. Figure 4 shows the geometric mean spectra of the scaled records.

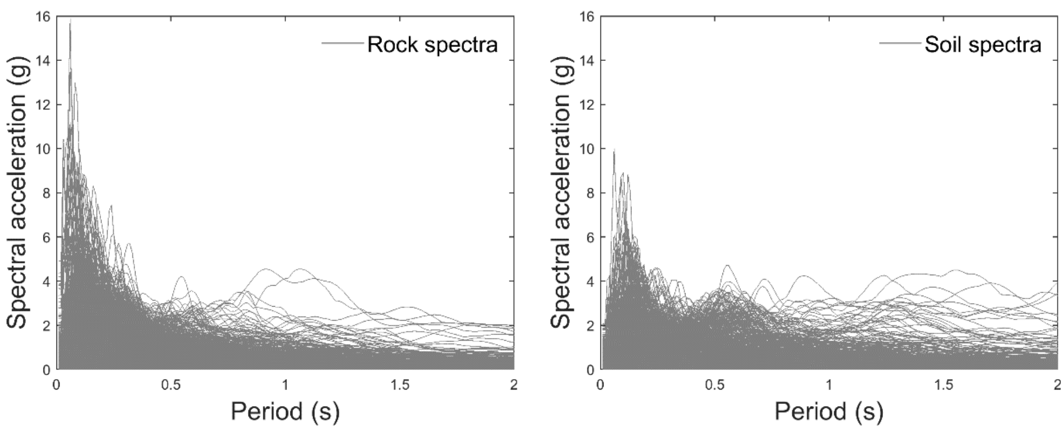

Figure 4: Scaled ground motion records (Left: Rock; Right: Soil)

4 FRAGILITY ASSESSMENT

Characterization of fragility is an important step in the probabilistic assessment of seismic risk. This section describes the development of fragility functions for the URMM housing typology. As mentioned above, these functions are derived from the dynamic response of SDoFs subjected to a large number of ground motion records from Colombia. The resulting fragility functions were compared with those proposed for this typology in previous research [5]. The derived set of functions has been used to assess the number of injuries due to earthquakes.

4.1 Intensity measures

IMs are parameters extracted from ground motion records. The most important property expected from IMs is their effectiveness in predicting EDPs. Ideally, an IM should contain enough information about the ground motion so that the structural response can be predicted with confidence. An IM that exhibits efficiency could potentially reduce the number of structural calculations in urban earthquake risk assessments. Several of the IMs used in this work are taken from those used in [15]. They have been used to predict the MGDR described in section 2.2.

4.2 Random characterization of the fundamental period of the analysed models (T_1)

Due to the probabilistic approach followed in this article, it is of paramount importance to generate a set of fundamental periods representing the analyzed typology. To do this, one can take advantage of classical relationships between the evolution of the fundamental period of the analyzed systems and a physical variable representing the height of the structure [2]. For the case of study, it has been considered the following formula to relate the fundamental period vs the height of the structure [8]:

$$T_1 = C_h * H^{0.75} \tag{9}$$

For the orthogonal direction (T_2), it has been assumed that the period value is obtained as a random fraction of T_1, which varies uniformly in the interval 0.75-1. To consider possible uncertainties in the characterization of T_1, it has been considered that C_h in equation (9) is a random term that depends on the type of structure. In the case of URMM typologies its average value is 0.09 and it has been assumed a coefficient of variation equal to 0.12. Figure 5 shows ten thousand realizations of T_1 according to the procedure described above. It can be seen the good agreement between the expected value of the generated models and equation (9).

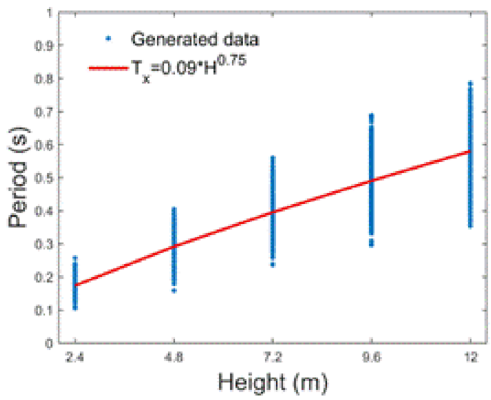

Figure 5: Relationship between $\boldsymbol{T_x}$ and H

Once both set of periods (T_1 and T_2) have been derived, the procedure described in section 2.2 has been applied to estimate MGDR as a random variable. Note that this calculation was performed for both types of ground motion records (recorded rock and soil locations). Since the number of generated models (ten thousand) significantly exceeds the number of ground motion records (one thousand and seven hundred for rock and soil, respectively), a random pairing between records and realizations of T_1 has been performed. In this way, the same ground motion record can be paired several times with realizations of T_1. Thus, the MGDR obtained for both type of records has been correlated with the IMs described in [15]. Figure 6 and Figure 7 show these relationships in the log-log space for ground motions recorded on Rock and Soil, respectively.

4.3 Efficiency

In this study, IM-EDP relationships have been characterized by means of nonlinear regression analyses in the log-log space. In this sense, the following general linear least-square model allows several types of regression:

$$y = \sum_{i=1}^{m+1} \alpha_{i-1} z_{i-1} + \varepsilon \tag{10}$$

where $\alpha_0, \alpha_1, \ldots \alpha_m$ are the coefficients providing the best fit between model and data; z_0, z_1, $\ldots z_m$ are basic functions; ε represents the residuals. It can easily be seen how polynomial regression falls within this model. That is, $z_0 = 1, z_1 = x, \ldots z_m = x^m$ [16]. Note that other nonlinear relationship can be used as z. Substituting in equation (10) $y = \ln EDP$ and $z_{i-1} = (\ln IM)^{i-1}$, the linear least-square model using polynomial functions can be used to extract statistical information from IM-EDP pairs according to the following equation (11):

$$\ln EDP = \sum_{i=1}^{m+1} \alpha_{i-1} (\ln IM)^{i-1} + \varepsilon \tag{11}$$

For $m=2$, equation (11) adopts the following quadratic form:

$$\ln EDP = \alpha_0 + \alpha_1 \ln(IM) + \alpha_2 \ln(IM)^2 + \varepsilon \tag{12}$$

where α_0, α_1 and α_2 are scalars maximizing the coefficient of determination, R^2, between IM-EDP pairs. This variable is generally used to quantify efficiency when analyzing IM-EDP pairs (see for instance Ebrahimian et al. 2015 [17]). For a perfect fit, R^2=1, signifying that the quadratic function explains 100% of the data variability. R^2 is used herein to provide an estimation of the variability when analyzing relationships involving IM-EDP pairs. That is, the higher R^2 the lower the variability when predicting some EDP given an IM. Consequently, the IM providing the highest R^2 will be the most efficient one, in the sense that it allows reducing the variability in seismic risk estimations.

4.4 Derivation of fragility functions

From a set of IM-EDP pairs, one can derive fragility functions according to the so-called 'cloud analyses approach [4]. This methodology requires calculating the best fit curve between a set of IM and EDP realizations in the log-log space. The resulting curve is used to estimate the mean value of a parametric statistical distribution, given an IM value. The variability of this parametric distribution ($S_{y/x}$) is estimated as the standard deviation of the IM-EDP residuals with respect to the fitted curve. In this way, the probability of exceeding a certain damage threshold can be calculated. These thresholds are realizations of the engineering demand parameter under consideration, EDP_C.

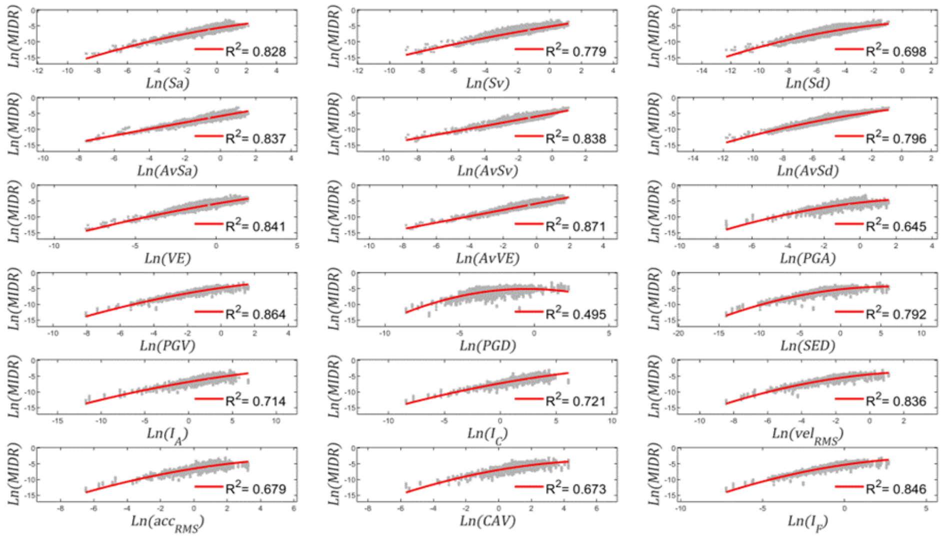

Figure 6: Ten-thousand IM-EDP pairs from URMM building models of one- to five-stories using ground mot

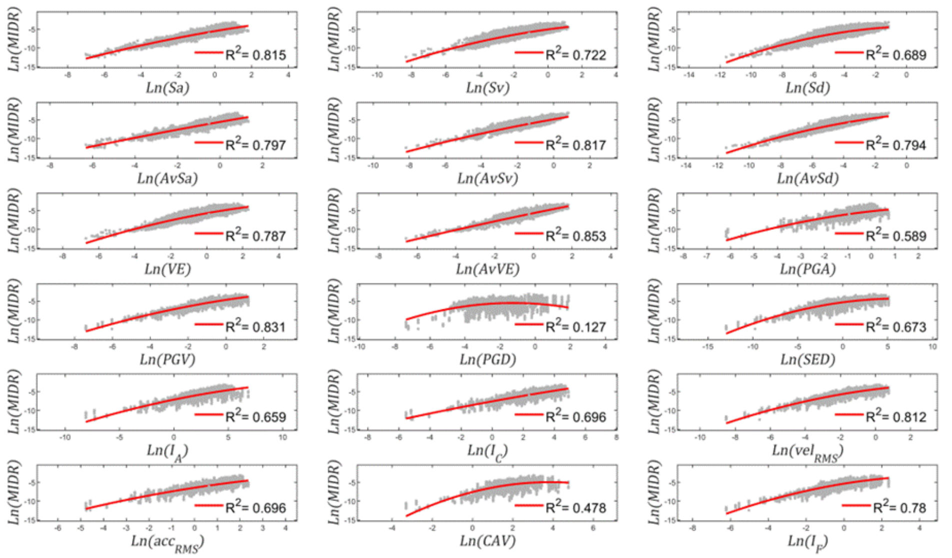

Figure 7: Ten-thousand IM-EDP pairs from URMM building models of one- to five-stories using ground mot

In this study, four damage states are considered, ranging from slight to complete damage; they are calculated by means of equation (13) to (16):

$$DS1 = 0.75\ \mathrm{Sd}_y \tag{13}$$

$$DS2 = 0.50\ \mathrm{Sd}_y + 0.33\ \mathrm{Sd}_u \tag{14}$$

$$DS3 = 0.25\ \mathrm{Sd}_y + 0.67\ \mathrm{Sd}_u \tag{15}$$

$$DS4 = \mathrm{Sd}_u \tag{16}$$

In these equations, Sd_y=0.12% (yielding displacement) and Sd_u =0.55% (ultimate displacement); these limits are obtained from [8,18–20]. Table 1 shows the calculated values according to equation (13) to (16).

	Slight (DS1)	Moderate (DS2)	Severe (DS3)	Complete (DS4)
Damage threshold	0.0009	0.0018	0.0039	0.0055

Table 1: Damage thresholds for URMM [5]

In this manner, fragility functions presented in Figure 8 have been derived by considering the damage thresholds shown in Table 1. It can be seen in these figures that fragility functions derived from records acquired on Soil tend to provide higher probabilities of damage. AvSv has been selected to derive these curves based on the average efficiency to predict the MGDR (see Figure 6 and Figure 7). In fact, this IM has been used not only to develop fragility functions for several damage thresholds but also to estimate the number of affected people according to Hazus 99 [21].

4.5 Validation of the fragility function

In order to validate the proposed methodology, a comparison has been made with fragility curves obtained in previous research for a similar structural typology [5]. Specifically, fragility curves derived for one-story URMM building have been extracted from this research. However, such curves have been obtained with respect to the spectral acceleration in a fundamental period equal to 0.3 seconds. In addition, it is worth mentioning that these curves consider that PF_1 is equal to 1.4. This differs from the hypothesis presented in this research regarding the evolution of PF_1 (see Figure 1). In spite of these differences, fragility functions based on $\mathrm{Sa}(T_1)$ have been calculated obtained considering the one-story simulated models.

From these data, two set of fragility functions are established to calculate damage probabilities. In the first case, it is assumed that the PF_1 is variable as a function of story height, as shown in section 2.2. In the second scenario, it is assumed that $PF_1 = 1.4$ and is constant for all the buildings. Figure 9 shows the curves obtained with the current model and the curves referred in Martins & Silva, 2021 [5]. It can be observed that, for the case 1 (left), the curves obtained with the current model exhibit a good fit with the reference ones for the slight and moderate damage states. For the severe and complete damage, the presented model provides lower probabilities of exceedance.

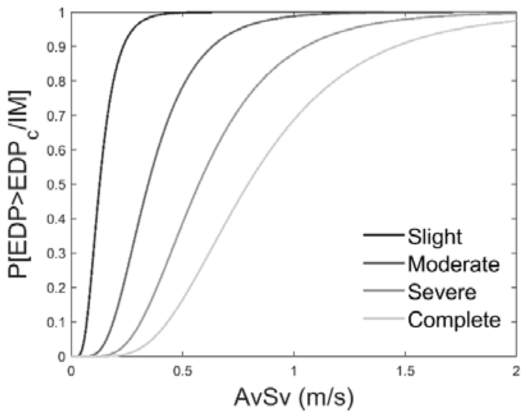

Figure 8: Fragility functions for URMM buildings. Left: Recorded on Rock. Right: recorded on Soil

For the second case (right), it can be observed that the modelled curves for the slight and moderate damage states show a tendency towards higher probability values whilst for severe and complete a good fit is observed.

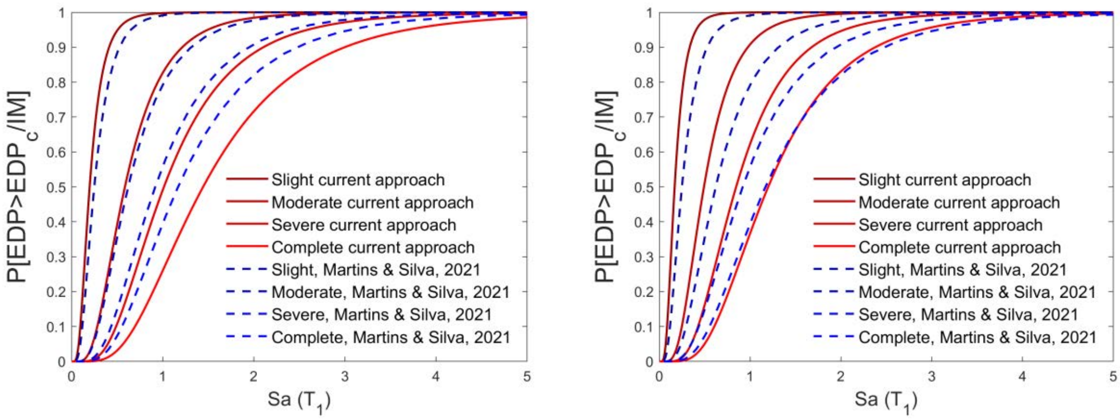

Figure 9: Capacity curves for current approach models (Red lines) and GEM models (Blue dashed lines). Left (Scenario 1): assumed that PF_1 is variable as a function of height. Right (Scenario 2): assumed that $PF_1 = 1.4$ is constant for all heights

To verify the performance of the fragility curves obtained, a comparison is made with a real disaster scenario such as the 1999 Armenian earthquake in Colombia [6]. Therefore, an evaluation is made between the real number of victims observed in the Armenia disaster and the number of victims simulated from the two hypotheses regarding PF_1 presented above. This allows to determine whether the developed model adapts to the real conditions of the affected area. Because of the soil conditions of the affected area, fragility functions derived for soil conditions have been employed. It is worth mentioning that the number of men reported suffering injury level 4 was equal 573, whilst on the women's site, this number was 731. In addition, the most affected structural typology during this catastrophe was URMM.

The most representative ground motion record of this earthquake was acquired at the Cordoba station. This record has been used as reference to estimate the expected intensities in terms of AvSv and the geometric mean spectrum. From this spectrum, AvSv= 0.617 m/s (the period intervals between 0.04 and 0.7 sec have been used to estimate this IM). The data on the population affected by this earthquake are taken from the DANE report [6], which states that during the state of emergency a total of 1304 deaths and disappearances were reported for the city of Armenia.

To estimate the number of people having injury level 4 by using the numerical approach of this research, the AvSv value (i.e. AvSv=0.617 m/s) is used to estimate damage probabilities. Based on this, the probability of occurrence of each damage state is estimated from the fragility functions presented in Figure 8, for records on soil (see Table 2).

	Slight	Moderate	Severe	Complete
Probability of occurrence	0.068	0.2357	0.2416	0.4543

Table 2: Probability of occurrence of each damage state given that AvSv=0.6 m/s

Based on these probabilities, and by considering that 214388 were the number of inhabitants in the city of Armenia for that time, Figure 10 shows a summary of the number of affected people discretized by gender and injury level. Also, this figure shows the results obtained for the two cases considered for validation. For the first case (Left), the number of affected people with injury level 4 is 1135.8. For the second case (Right), a total of 1394.6 suffered injury level 4.

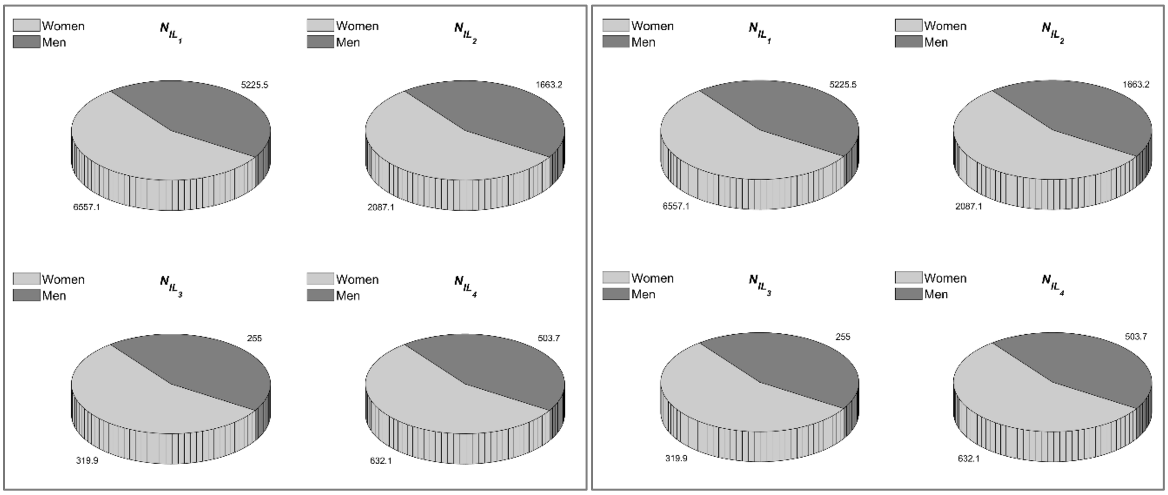

Figure 10: Simulation of the number of affected people in the Armenia's catastrophe. Left (Scenario 1): assumed that PF_1 is variable as a function of height. Right (Scenario 2): assumed that $PF_1 = 1.4$ is constant for all heights.

If the total number of casualties, calculated from the simulations (Case 1: 1135.8 people; Case 2: 1394.6 people), is compared with those presented in the DANE's report (1304 people) [6], it can be seen that the second case provides values more similar to those reported for the disaster zone. However, it must be considered that the generated data are based on URMM typology, and they do not reflect other factors that trigger variations, for example, other typologies that are less frequent but more prone to damage can modify this estimate. In this case, data on the number of inhabitants living in different types of family housing should be included in the analysis. In the DANE's report [6], it can be seen that this typology (URMM) was not the only one that collapsed, so it would not be appropriate to attribute all the risk to this typology. In line with the above, it is decided to opt for the first hypothesis, as it presents more conservative values that are more in line with this scenario. Anyhow, both hypothesis (Case 1 and Case 2) provides very satisfactory results.

5 CONCLUSIONS

For this study, a highly vulnerable structural typology (URMM) has been studied. Note that despite the high vulnerability of this typology, it is present in most countries of the world. In fact, several global earthquake-related catastrophes may be associated with the use of this type of vulnerable housing [3].

A fragility model based on the contribution of several SDoF systems, whose vibration periods are around the fundamental one for this typology, has been developed in this research. To do so, a set of ground motions recorded in Colombia has been used to represent seismic hazard. The cloud analysis has been employed to derive the fragility functions [4]. Based on these curves, the expected risk in terms of injuries has been estimated for two cases, one for a PF_1 variable as a function of the number of stories and another one assuming that PF_1 remains constant. Then, the Hazus methodology has been applied to assess the expected risk in terms of number and severity of injured [21]. The results were compared with the data obtained after the Armenia disaster [6] and it was found that although the two cases produced congruent and fairly accurate data, Case 1 presents the most conservative data. The variation can easily be attributed to various external factors such as other types of structures that could potentially fail and have not been considered.

It was also possible to estimate the influence of soil conditions on the quantification of expected risk. It has been observed that the expected risk increases when records obtained from soil sites are used in the calculation. This can be explained by considering the results shown in Figure 3. That is, the spectral ordinates are higher in soil than in rock records when comparing the same percentiles of the analyzed data. This difference becomes more evident as the percentile increases.

In terms of future research activities, it will be interesting to recalculate the fragility functions by disaggregating the results based on the number of stories. It is expected that results based on this classification will be more reliable. In addition, it has been observed that IMs based on energy are more efficient than those based on acceleration (at least when the entire set of models is considered simultaneously). Regarding the structural typology analyzed, it has been confirmed its low performance in front of ground motion records induced by earthquakes. Further research should be oriented to provide a rapid and economic solution to diminish the vulnerability of this type of structures.

This research should not stop here. Note that the proposed model easily allows the implementation of new structural typologies if relationships between the fundamental period and the height of the structure are available. In this sense, most of the existing typologies have this information [2].

6 ACKNOWLEDGMENT AND FUNDING

This research has been partially funded by the Spanish Research Agency (AEI) of the Spanish Ministry of Science and Innovation (MICIN) through project with reference: PID2020-117374RB-I00/AEI/10.13039/501100011033.

7 REFERENCES

[1] Y.F. Vargas-Alzate, L.G. Pujades, J.R. González-Drigo, R.E. Alva, L.A. Pinzón, On the equal displacement aproximation for mid-rise reinforced concrete buildings, in: Proceedings of the 7th International Conference on Computational Methods in Structural Dynamics and Earthquake Engineering (COMPDYN 2015), Institute of Structural Analysis and Antiseismic Research School of Civil Engineering National Technical University of Athens (NTUA) Greece, Athens, 2019: pp. 5490–5502. https://doi.org/10.7712/120119.7321.19849.

[2] R.K. Goel, A.K. Chopra, Period Formulas for Moment-Resisting Frame Buildings, Journal of Structural Engineering. 123 (1997) 1454–1461. https://doi.org/10.1061/(ASCE)0733-9445(1997)123:11(1454).

[3] S. Brzev, M. Tomaževič, M. Lutman, M. Bostenaru Dan, D. D'Ayala, M. Greene, The World Housing Encyclopedia: An Online Resource on Housing Construction in High Seismic Risk Areas of the World., (2003). http://db.world-housing.net/building/10/

[4] F. Jalayer, R. De Risi, G. Manfredi, Bayesian Cloud Analysis: Efficient structural fragility assessment using linear regression, Bulletin of Earthquake Engineering. 13 (2015) 1183–1203. https://doi.org/10.1007/S10518-014-9692-Z.

[5] L. Martins, V. Silva, Development of a fragility and vulnerability model for global seismic risk analyses, Bulletin of Earthquake Engineering. 19 (2021) 6719–6745. https://doi.org/10.1007/s10518-020-00885-1.

[6] DANE, Dimensión social y económica de los efectos del terremoto del eje cafetero. Diagnóstico para la reconstrucción, Santafé de Bogotá, 1999.

[7] E. Alarcón, Benito-Oterino M.B., Mucciarelli M., Liberatore D., Bulletin of Earthquake Engineering - v. 12, n. 5, Structurae. (2013) 1871–2298. https://structurae.net/en/literature/periodicals/bulletin-of-earthquake-engineering/20473-12-5

[8] N. Tarque, H. Crowley, R. Pinho, H. Varum, Displacement-Based Fragility Curves for Seismic Assessment of Adobe Buildings in Cusco, Peru, Earthquake Spectra. 28 (2012) 759–794. https://doi.org/10.1193/1.4000001.

[9] Freeman, Development and Use of Capacity Spectrum Method. Proceedings of the 6th U.S. National Conference on Earthquake Engineering, Seattle, Oakland, USA., in: Scientific Research Publishing, 1998. https://www.scirp.org/(S(351jmbntvnsjt1aadkposzje))/reference/ReferencesPapers.aspx?ReferenceID=1773086

[10] Applied Technology Council, ATC-40 Seismic evaluation and retrofit of concrete buildings, Applied Technology Council, Redwood City, California , 1996.

[11] SGC, Sistema de Consulta de la Amenaza Sísmica de Colombia, Colombian Geological Survey. (2020). https://amenazasismica.sgc.gov.co/.

[12] W.A.S., H.A., B.J.W., B.J. and G.D.N. Haselton C.B., Selecting and Scaling Earthquake Ground Motions for Performing Response-History Analyses , 15th World Conference on Earthquake Engineering, Lisboa, Portugal. (2012).

[13] N. Luco, P. Bazzurro, Does amplitude scaling of ground motion records result in biased nonlinear structural drift responses?, Earthq Eng Struct Dyn. 36 (2007) 1813–1835. https://doi.org/10.1002/EQE.695.

[14] Y.F. Vargas-Alzate, R. Gonzalez-Drigo, J.A. Avila-Haro, Multi-Regression Analysis to Enhance the Predictability of the Seismic Response of Buildings, Infrastructures (Basel). 7 (2022) 51. https://doi.org/10.3390/infrastructures7040051.

[15] Y.F. Vargas-Alzate, J. Hurtado, Efficiency of Intensity Measures Considering Near- and Far-Fault Ground Motion Records, Geosciences (Basel). 11 (2021) 234. https://doi.org/10.3390/geosciences11060234.

[16] S.C. Chapra, Applied numerical methods with MATLAB® for engineers and scientists, Fourth, New York, NY: McGraw-Hill Education, 2018.

[17] H. Ebrahimian, F. Jalayer, A. Lucchini, F. Mollaioli, G. Manfredi, Preliminary ranking of alternative scalar and vector intensity measures of ground shaking, Bulletin of Earthquake Engineering. 13 (2015) 2805–2840. https://doi.org/10.1007/s10518-015-9755-9.

[18] N. Tarque, H. Crowley, R. Pinho, H. Varum, Seismic risk assessment of adobe dwellings in Cusco, Peru, based on mechanical procedures | Semantic Scholar, 14th European Conference on Earthquake Engineering Ohrid, North Macedonia. (2010).

[19] F. De Luca, G.M. Verderame, Seismic Vulnerability Assessment: Reinforced Concrete Structures, in: Encyclopedia of Earthquake Engineering, Springer Berlin Heidelberg, Berlin, Heidelberg, 2015: pp. 3182–3210. https://doi.org/10.1007/978-3-642-35344-4_252.

[20] G. Karanikoloudis, P.B. Lourenço, Structural assessment and seismic vulnerability of earthen historic structures. Application of sophisticated numerical and simple analytical models, Eng Struct. 160 (2018) 488–509. https://doi.org/10.1016/j.engstruct.2017.12.023.

[21] FEMA, HAZUS Earthquake Loss Estimation Methodology. Technical Manual, Prepared by the National Ins- titute of Building Sciences for the Federal Emergency Management Agency, Washington D.C., 1999.